Poly(vinyl pyrrolidone)-Assisted Sol−Gel Deposition of Quality β-Barium Borate Thin Films for Photonics Applications

C. Lu, S. S. Dimov, and R. H. Lipson*

Department of Chemistry, University of Western Ontario, London, Ontario N6A 5B7, Canada

Received April 16, 2007. Revised Manuscript Received July 18, 2007

β-Barium borate (β-BaB_2O_4, β-BBO) films were deposited on fused silica substrates by spin coating poly(vinyl pyrrolidone) (PVP)-modified metallo-organic solutions. Film thicknesses of more than 500 nm were obtained by a single spin-coating step followed by O_2 plasma and thermal treatments. Crack formation was effectively suppressed by the introduction of PVP. Samples annealed at 650 °C exhibit high transparency over a wide wavelength range (1100 nm−210 nm) and have a preferred orientation corresponding to the (006) crystallographic direction. The increased thickness of the BBO films provided a >10-fold increase in the second harmonic generation (SHG) efficiency when compared to BBO layers fabricated without the addition of PVP and O_2 treatment. The precursor gels are readily amenable to contact lithography leading to patterned β-BBO films.

1. Introduction

β-Barium borate (β-BBO, β-BaB_2O_4) is a well-known nonlinear optical material with a high second-order nonlinear susceptibility ($d_{eff} \sim 2.2$ pm/V), wide transparency range (189 nm−3500 nm), and high damage threshold.[1,2] Single crystals have long been incorporated into commercial laser systems as components for frequency doubling or tripling and as the main nonlinear element in optical parametric oscillators (OPO) pumped by a UV laser.[3] Thin films of β-BBO can be used in compact optical systems as frequency converters, waveguides,[4] and switches. The nonlinear efficiency of the film is determined by both its crystallinity and orientation and by its geometrical structure if fabricated as a photonic crystal.[5]

Wet deposition methods have been extensively used to produce β-BBO thin films with a preferred (00*l*) orientation.[6−10] Typically, however, only <100 nm thick crack-free films can be obtained by single-step sol−gel or chemical solution deposition methods. While thicker films can be obtained by a multiple coating−annealing process, such a repetitive procedure is both time-consuming and can introduce random islands which are created by crystal beads formed during each deposition and annealing step. More significantly, the optical properties (transparency and second harmonic generation (SHG) efficiency) of the films deteriorate as residual absorbing carbon deposits produced during annealing accumulate.[6,11]

In principle, the ceramic film thickness can be increased by starting with solutions having higher precursor concentrations. These however, tend to crack.[12,13] Thus, methods are needed to produce high optical quality but thicker films of β-BBO which can be fabricated as and/or integrated into photonic devices.

Poly(vinyl pyrrolidone) (PVP) is a water-soluble polymer made from the *N*-vinyl pyrrolidone monomer which has been used as an additive in sol−gel methods to produce thick crack-free films (≥1.0 μm) of ferroelectrics such as $BaTiO_3$ and Pb(Zr,Ti)O_3 (PZT).[12,14−16] In this work, β-BBO films have been prepared for the first time using a PVP-modified sol−gel method. The thicknesses of the BBO films were found to increase by a factor >6 in a single spin-coating step, while maintaining a (006) crystal orientation. The resultant β-BBO films exhibit very high SHG efficiencies.

2. Experimental Section

Boron ethoxide and metal barium were used as the starting source for B and Ba, respectively. Ba metal chips were first added to anhydrous ethanol to form a barium ethoxide solution. A stoichiometric aliquot of boron ethoxide was then added drop-wise while stirring vigorously. The resultant solution was diluted by the mixture solution of ethanol (EtOH) and 2-ethoxide ethanol (2EtOEtOH)

* Corresponding author. E-mail: rlipson@uwo.ca.

(1) Eimerl, D.; Davis, L.; Velsko, S.; Graham, E. K.; Zalkin, A. *J. Appl. Phys.* **1987**, *62*, 1968.
(2) Nikogosyan, D. N. *Appl. Phys. A* **1991**, *A52*, 359.
(3) Goodno, G. D.; Guo, Z.; Miller, R. J. D.; Miller, I. J.; Montgomery, J. W.; Adhav, S. R.; Adhav, R. S. *Appl. Phys. Lett.* **1995**, *66*, 1575.
(4) Degl'Innocenti, R.; Guarino, A.; Poberaj, G.; Gunter, P. *Appl. Phys. Lett.* **2006**, *89*, 041103/1.
(5) Soljacic, M.; Joannopoulos, J. D. *Nat. Mater.* **2004**, *3*, 211.
(6) Neves, P. P.; Maia, L. J. Q.; Bernardi, M. I. B.; Zanatta, A. R.; Mastelaro, V. R.; Zanetti, S. M.; Leite, E. R. *J. Sol-Gel Sci. Technol.* **2004**, *29*, 89.
(7) Kobayashi, T.; Ogawa, R.; Kuwabara, M. *Mater. Lett.* **2003**, *57*, 1056.
(8) Yogo, T.; Niwa, K.; Kikuta, K.-I.; Ichida, M.; Nakamura, A.; Hirano, S.-I. *J. Mater. Chem.* **1997**, *7*, 929.
(9) Yogo, T.; Kikuta, K.; Niwa, K.; Ichida, M.; Nakamura, A.; Hirano, S.-I. *J. Sol-Gel Sci. Technol.* **1997**, *9*, 201.
(10) Kobayashi, T.; Ogawa, R.; Miyazawa, K. I.; Kuwabara, M. *J. Mater. Res.* **2002**, *17*, 844.
(11) Nie, W.; Lurin, C.; Paz-Pujalt, G. R. *SPIE Vol. 1758* (Sol-Gel Opt. II), **1992**, 284.
(12) Kozuka, H.; Higuchi, A. *J. Am. Ceram. Soc.* **2003**, *86*, 33.
(13) Scherer, G. W. *J. Non-Cryst. Solids* **1992**, *147−148*, 363.
(14) Kozuka, H.; Kajimura, M.; Hirano, T.; Katayama, K. *J. Sol-Gel Sci. Technol.* **2000**, *19*, 205.
(15) Kozuka, H.; Kajimura, M. *Chem. Lett.* **1999**, 1029.
(16) Kozuka, H.; Takenaka, S.; Tokita, H.; Okubayashi, M. *J. Eur. Ceram. Soc.* **2004**, *24*, 1585.

10.1021/cm071037m CCC: $37.00
Published on Web 09/07/2007

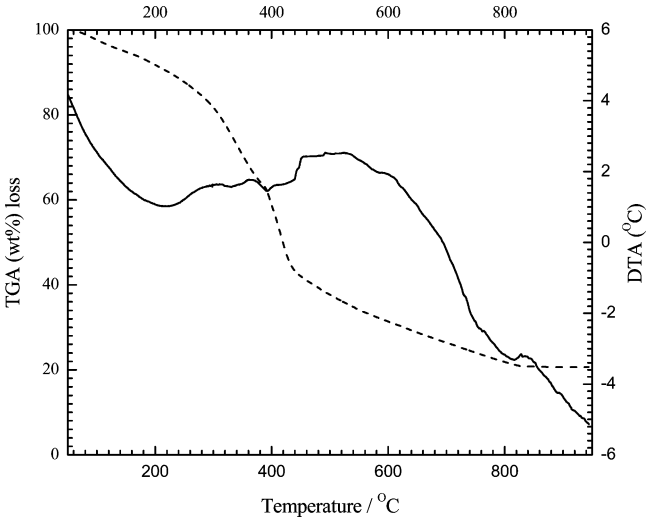

Figure 1. TGA (dashed line) and DTA (solid line) curves of the precursor powder used to make PB8 thin film. The heating was done in air at a heating rate of 5 °C/min.

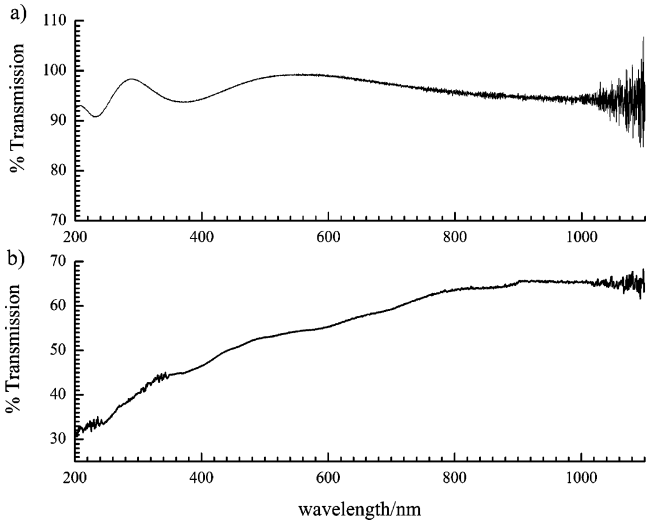

Figure 2. (a) UV−visible transmission spectrum of a PB8 β-BBO film on fused silica, annealed at 650 °C for 1 h. The transmission through bare fused silica was set as the baseline. (b) UV−visible transmission spectrum of a β-BBO film made without an O_2 plasma treatment.

(V_{EtOH}/ $V_{2EtOEtOH}$ = 10:1) to produce a concentration of 0.2 M. The mixture solution was then refluxed at 80 °C for 16 h. Afterward, 0.8% (wt %) of PVP (MW ≈ 360 000) was added, and the mixture was stirred for 2 h to form the final viscous homogeneous precursor solution.

The viscous precursor solution was spin cast at 1000 rpm onto a fused silica substrate for 1 min. The ∼1 cm^2 films obtained were prebaked at 150 °C for 30 min to remove any residual solvent and then hydrolyzed at 250 °C using a gas mixture of water vapor and air (air bubbled through water at ∼50 °C) for 1 h to form low-temperature γ-phase BBO. The films were then O_2 plasma treated to break the PVP chains down into smaller more volatile species. Last, the film was annealed at higher temperature for 1 h to induce a phase change to the crystalline β-BBO phase.

The films were characterized by a number of techniques including thermogravimetric analysis (TGA), differential thermal analysis (DTA), transmission spectroscopy, and power X-ray diffraction (XRD) using a Co source (λ = 1.792 Å). Images were obtained using a scanning electron microscope (SEM) located in the Nanofabrication Facility of the Physics and Astronomy department at the University of Western Ontario.

3. Results and Discussion

(a) Film Characterization. The β-BBO films formed using PVP were compared to those fabricated by established sol−gel methods[8,9] using identical concentrations of the gel precursor. Thin film samples prepared using 0.8 wt % and 2.0 wt % PVP are labeled in this work as PB8 (0.8%) and PB20 (2%), respectively. The film prepared without PVP is labeled PB0.

Precursor powders were obtained by drying the solution at 150 °C to remove the solvent. Figure 1 shows the TGA and DTA curves of the powder made with 8 wt % PVP but untreated by an O_2 plasma. Several major weight losses are observed by TGA. The weight loss below 210 °C is attributed to the evaporation of any remaining solvent, while the weight loss between 210 °C and 390 °C is most likely due to the decomposition and removal of organic groups such as EtO− and 2-EtOEtO−.[17] The PVP begins to decompose at 390 °C. The complete decomposition and removal of the PVP residue is not completed until the temperature reaches 800 °C. No further weight loss is observed at higher temperatures. In total, the TGA curve indicates an 80% weight loss.

The DTA curve exhibits one exothermic peak at 830 °C that is assigned to the phase transition from β-BBO to α-BBO. On the basis of previous reports,[8,9] the phase transition from the low-temperature γ-phase to β-BBO without PVP addition takes place around 600−700 °C. In this work, the broad peak between 300 °C and 800 °C in the DTA curve is due to the decomposition of PVP which makes it difficult to determine the exact phase transition temperature for the composite system. Carbon produced by the decomposition of PVP generated blackish color on the surface of the sample (powder and film), which seriously deteriorated the quality of the BBO sample. The blackish color persisted even after heating the sample at 700 °C for 24 h.

Carbon is always generated in β-BBO thin films fabricated by sol−gel methods[6] and is extremely difficult to remove. An O_2 plasma[18−20] was therefore implemented to remove organic remnants at low temperatures. O_2 plasmas are often used to ash the substrates of micro-electro-mechanical systems (MEMS) and clean away all organic residues on their surfaces.

In this work, most of the PVP and other organic residues could be removed after 10−20 min of O_2 plasma treatment. A transmission spectrum of a PB8 film after heating at 650 °C for 1 h is shown in Figure 2a). The film is transparent between 1100 and 210 nm. In contrast, the transparency of β-BBO films made without O_2 plasma pretreatment is substantially reduced due to the presence of carbon deposits (Figure 2b).

(17) Chen, S.-Y.; Chen, I. W. *J. Am. Ceram. Soc.* **1994**, *77*, 2337.
(18) Worsley, M. A.; Bent, S. F.; Fuller, N. C. M.; Dalton, T. *J. Appl. Phys.* **2006**, *100*, 083301.
(19) Yonekura, K.; Sakamori, S.; Goto, K.; Matsuura, M.; Fujiwara, N.; Yoneda, M. *J. Vac. Sci. Technol., B* **2004**, *22*, 548.
(20) Tanaka, K.; Inomata, T.; Kogoma, M. *Plasmas Polym.* **1999**, *4*, 269.

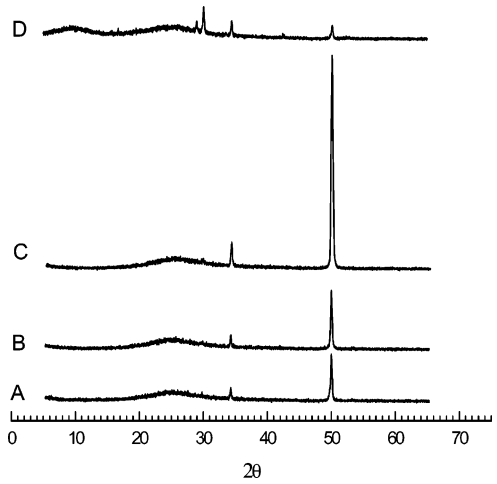

Figure 3. XRD spectra of BBO films after thermal treatment at 650 °C. (A) PB0 film made without O_2 plasma treatment, (B) PB0 film made after O_2 plasma treatment, (C) PB8 film made after O_2 plasma treatment, and (D) a PB20 film made after O_2 plasma treatment.

The XRD spectra of the PBO thin films with and without O_2 plasma treatment are similar (Figure 3, traces A and B). The results in Figure 3 indicate that the O_2 plasma treatment does not introduce or induce chemical changes in the films. The dominant feature at $2\theta \sim 50°$ corresponds to the (006) crystallographic plane. β-BBO has a lattice structure consisting of layers made of Ba^{2+} and anionic $(B_3O_6)^{3-}$ rings normal to the *c*-axis.[1] A (006) orientation corresponds to the situation where the *c*-axis lies perpendicular to the $(B_3O_6)^{3-}$ rings, and the rings are aligned in the plane of the film.

The absolute XRD (006) peak intensity for the PB8 sample is considerably higher than that obtained for the sample made without PVP (Figure 3, trace C) due to the enhanced thickness of the gel precursors prepared using PVP. In these experiments the thickest films that could be made without the addition of PVP were ~80 nm. Still, the addition of too much PVP adversely affects the crystallinity of the material as shown in Figure 3, trace D, for the PB20 film.

An SEM image of the PB0 thin film is shown in Figure 4a). Film cracking creates a mosaic pattern with typical domain sizes of 5−10 μm in length. Cracking is attributed to the internal stresses that result when the films are heat-treated. As the films adhere to the substrate, they can no longer contract along the directions parallel to the substrate surface. The resultant tensile stress produces the cracks observed.[7,12,14]

In contrast to PB0, the PB8 film is crack-free over its entire surface (Figure 4b). This smoothness exists even on the nanometer scale (Figure 4c). A film thickness of >500 nm was measured by using a focused ion beam (FIB) to mill out a cross-sectional area of the film (Figure 4d). Thus, the introduction of PVP increases the thickness of the films by more than a factor of 6. This thickness agrees with optical ellipsometry measurements which also gave an effective refractive index for the film of ~1.66 at 632 nm. This value is similar to that determined for bulk β-BBO.[2] The increased thickness correlates with the increased viscosity of the precursor solution.[15]

Although thin film thicknesses of >900 nm can be achieved in a single step by increasing the PVP concentration

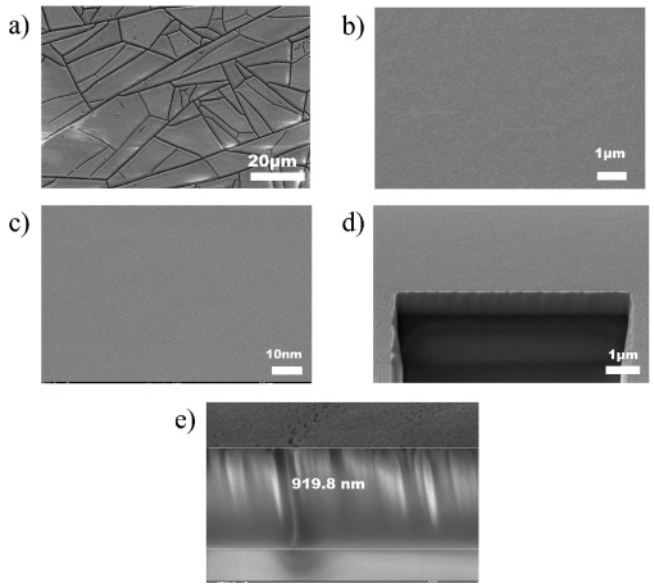

Figure 4. SEM images of BBO films thermal treated at 650 °C. (a) A PB0 film, (b) a PB8 film, (c) a PB8 film under high magnification, (d) a cross-sectional view of a PB8 film showing a thickness > 500 nm, and (e) a cross-sectional view of a PB20 film showing the porous surface morphology and a thickness > 900 nm.

further, as shown in Figure 4e for the PB20 sample, nanopores begin to develop, and there is a loss of crystallinity which degrades the nonlinear optical properties of the film. Instead, 1 μm films are best obtained by repeating the synthesis twice under the optimum conditions.

One important metric is the extent that (006) is the preferred orientation of the films as this is expected to have a strong effect on their nonlinear efficiency. The degree of orientation[7] was found from the XRD spectra to be ~90% for both the PB0 and the PB8 films. The PB20 films were substantially less orientated, exhibiting only a 15% preference for the (006) plane. These results indicate that the addition of 8% PVP has no effect on the orientation of the β-BBO but still dramatically improves the morphology of the films. This is consistent with previous work where PVP was used as a stress-relaxing agent in the formation of ceramic films.[13,14] Here, PVP was thought to slow condensation reactions in the gel and promote structural relaxation.

The XRD patterns of the PB8 films annealed at different temperatures are shown in Figure 5. Below 550 °C the BBO film is in an amorphous state. The conversion to the β-phase begins around 600 °C. Three small peaks attributed to (113) plane at $2\theta = 29.6°$, the (104) plane at $2\theta = 34.2°$, and the (006) plane at $2\theta = 50°$ are clearly observed. The (006) orientation dominates at 650 °C but then decreases at higher temperatures. Small XRD features attributed to the conversion of β-BBO to the α-phase appear (2θ at 26.8° and 45.8° due to the (018) and (214) planes, respectively) when the sample is annealed at 750 °C. At 800 °C, the film is completely converted to α-BBO. These results are consistent with the TGA and DTA analyses.

(b) Nonlinear Optical Characterization. The quality of the films was also assessed by measuring SHG signals obtained by irradiating the samples using the infrared fundamental beam at 1064 nm generated by a Nd:YAG laser (Spectra-Physics Pro-250, 20 Hz repetition rate, 4 ns/pulse).

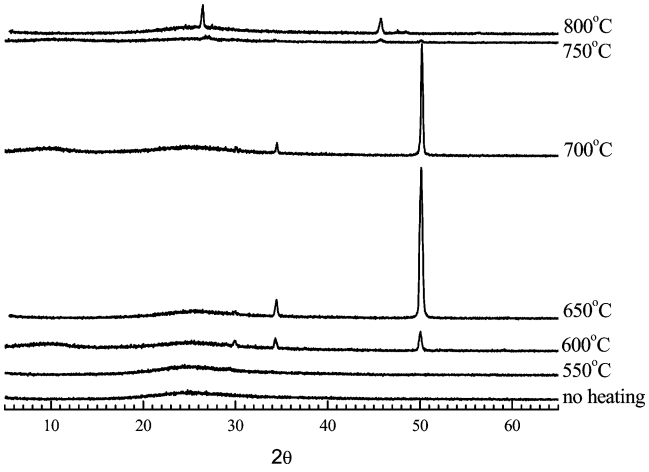

Figure 5. XRD patterns of a PB8 film baked at different temperatures for 1 h.

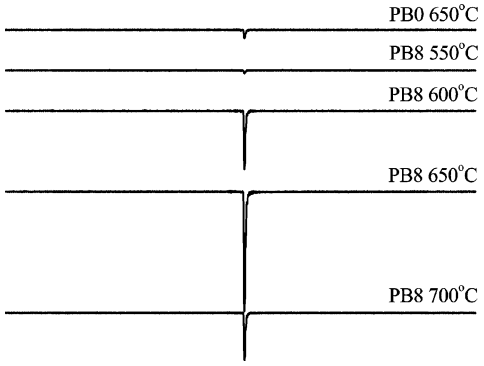

Figure 6. SHG response of PB8 β-BBO films as a function of annealing temperature. The top trace is the SHG signal of a PB0 film annealed at 650 °C. The *y*-axis is the intensity of the SHG signal plotted on the same scale for each graph.

The SHG signal was dispersed from the fundamental beam using an infrared cutoff filter in front of a monochromator, detected with a photomultiplier, and monitored on a digital oscilloscope (Tektronix, TDS744A). The SHG response of a β-BBO PB8 thin film is shown in Figure 6 as a function of annealing temperature. The SHG efficiency correlates strongly with the intensity of (006) peak in the XRD spectra which is a maximum for PB8 at 650 °C. Not surprisingly, this shows that the nonlinear response of the thin film depends critically on its crystallinity. Again, this enhancement is due to the increased film thickness and more uniform morphology. The decrease in the SHG signal at 700 °C is due to the conversion of β-BBO to the inactive α-phase. The SHG is also >10× more efficient than that for films made without PVP and annealed at 650 °C (the PB0 trace in Figure 6).

The effective second-order nonlinear coefficient, d_{eff}, for the β-BBO thin films was evaluated by performing SHG measurements and comparing those results with the SHG response of a Y-cut quartz crystal plate (CVI, 0.690 mm thick).[21] In each set of measurements, the BBO and quartz reference samples were tilted and rotated with respect to the incident beam axis to attain the maximum SHG efficiency.

The SHG intensity, $I(2\omega)$, generated from either the quartz or the BBO sample by a fundamental beam with intensity $I(\omega)$ is given by[21,22]

$$I(2\omega) \propto \left(\frac{\ell_s^2 I^2(\omega) d_{eff}^2}{n^2(\omega)\, n(2\omega)}\right) \frac{\sin^2\left(\frac{\pi \ell_s}{2\ell_c}\right)}{\left(\frac{\pi \ell_s}{2\ell_c}\right)} \quad (1)$$

where ℓ_s is the thin film thickness, $n(\omega)$ and $n(2\omega)$ are the film indices of refraction at frequency ω and 2ω, respectively, and ℓ_c is the coherence length of the film. Because the coherence length, defined by $\ell_{c,BBO} = \lambda/(4[n(\omega) - n(2\omega)]) \sim 16\ \mu$m for β-BBO is much larger than the film thickness ℓ_{BBO}, the factor $\sin^2(\pi\ell_{BBO}/2\ell_{c,BBO})/(\pi\ell_{BBO}/2\ell_{c,BBO})^2 \approx 1$. This approximation, however, cannot be made for the quartz plate because its coherence length (∼20 μm) is much less than the plate thickness.

In the calculation of the SHG intensity ratio between β-BBO and quartz plate, $I_{BBO}(2\omega)/I_Q(2\omega)$, where the subscript Q denotes quartz, the ratio $n_{BBO}(\omega)^2\, n_{BBO}(2\omega)/[n_Q(\omega)^2\, n_Q(2\omega)] \sim 1.25$. Therefore, the intensity ratio can be written as

$$\frac{I_{BBO}(2\omega)}{I_Q(2\omega)} \approx \left(\frac{\ell_{BBO}}{\ell_Q}\right)^2 \left(\frac{T d_{eff}^2}{1.25 d_{11,Q}^2}\right) \left(\frac{\left(\frac{\pi \ell_Q}{2\ell_{c,Q}}\right)^2}{\sin^2\left(\frac{\pi \ell_Q}{2\ell_{c,Q}}\right)}\right) \quad (2)$$

where $d_{11,Q} = 0.34$ pm/V is the second-order nonlinear coefficient of quartz and T represents the measured transmission of the sample (measured to be 0.9 in these experiments). Equation 2 can be rearranged to yield the following expression for d_{eff}:

$$d_{eff} \approx \left(\frac{\ell_Q}{\ell_{BBO}}\right) \left(\frac{1.25 I_{BBO}}{T I_Q}\right)^{1/2} d_{11,Q} \frac{\sin\left(\frac{\pi \ell_Q}{2\ell_{c,Q}}\right)}{\left(\frac{\pi \ell_Q}{2\ell_{c,Q}}\right)} \quad (3)$$

The maximum values of d_{eff} for the PB0 and PB8 films were calculated using eq 3 to be 1.6−1.8 pm/V and 1.7−1.9 pm/V, respectively. These results are similar to those reported for thin β-BBO films elsewhere and are comparable to the d_{22} value of the bulk crystal (=2.2 pm/V).[23] The differences in the d_{eff} values for the PB0 and PB8 films are not very large which indicates that the SHG enhancement measured for PB8 is due to the increased thickness of the film.

(c) Patterning β-BBO Films by Contact Lithography. The fabrication of patterned β-BBO films by contact lithography now becomes a possibility because the addition of PVP leads to thicker β-BBO films and a more viscous gel precursor. This represents a significant advance because

(21) Shen, Y. R. *The Principles of Nonlinear Optics*; Wiley: New York, 1984; p 98.

(22) Lu, H. A.; Wills, L. A.; Wessels, B. W.; Lin, W. P.; Zhang, T. G.; Wong, G. K.; Neumayer, D. A.; Marks, T. J. *Appl. Phys. Lett.* **1993**, *62*, 1314.

(23) Maia, L. J. Q.; Feitosa, C. A. C.; De Vicente, F. S.; Mastelaro, V. R.; Siu Li, M.; Hernandes, A. C. *J. Vac. Sci. Technol., A* **2004**, *22*, 2163.

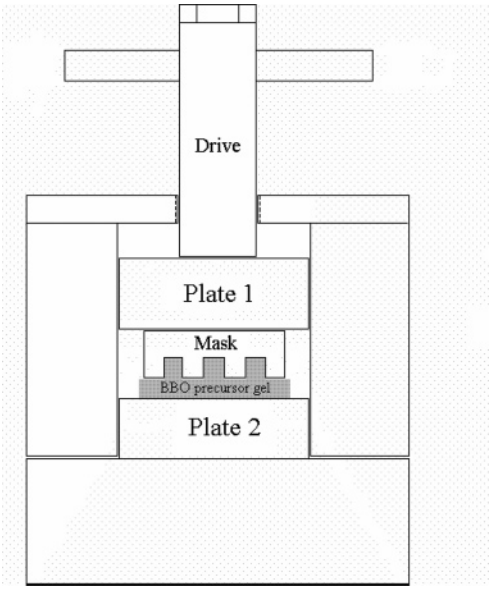

Figure 7. Schematic of the press used for contact lithography

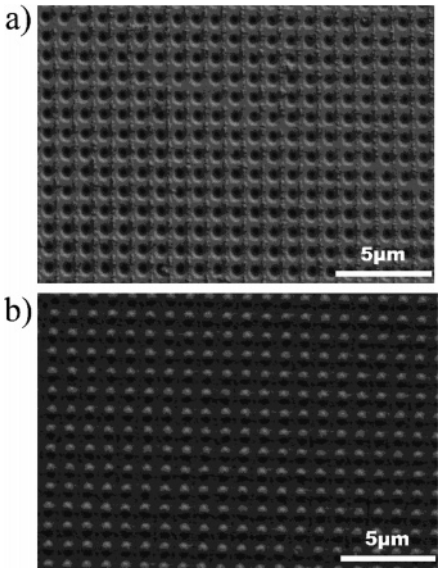

Figure 8. SEM images of (a) the Si mask used for contact lithography and (b) the patterned β-BBO (PB8) film.

the β-phase of the hygroscopic BBO inorganic salt is formed at a temperature which lies lower than its melting point[6] and, once formed, is not easily patterned using standard methods of patterning such as interference lithography combined with reactive ion etching (RIE)[24] or contact lithography.[25]

Contact lithography was carried out using the press shown schematically in Figure 7. Essentially the device is two pieces of highly polished steel plates (1.5 in. in diameter) separated by a distance which can be controlled and finely adjusted using a screw. This design allows the pressure applied to the sample to be reproducibly measured using a torque wrench. A two-dimensional mask with a hole periodicity of 1 μm and hole depth of 1 μm was fabricated in Si by a two-step process where interference lithography was first used to form a template in an organic photoresist, followed by RIE (Figure 8a). The PB8 film (without baking) and mask were placed inside the press and brought into contact with each other by adjusting the position of the screw. The press assembly was then transferred to an oven and heated to 100 °C. The heating expanded the metal plates which provided a more intimate contact between the mask and the gel. After 10 min, the oven was cooled to room temperature and the press was removed. The Si mask could then be peeled off and reused if desired. The patterned gel precursor was then heated to high temperatures to form the β-BBO phase (confirmed by XRD). A SEM image of the resultant inverse pattern is shown in Figure 8b). The quality of the structure is excellent in that the periodicity is preserved by the masking and baking processes. The spin-coated gel precursor is thicker than the final BBO film due to shrinkage during the heating process. An optimization of the process targeting the limits of achievable depth and periodicity for one-dimensional and two-dimensional structures is underway. Nevertheless, these initial results are encouraging.

4. Conclusions

β-BBO films have been made using a PVP-modified sol−gel synthesis involving an O_2 plasma treatment. Smooth crack-free films with excellent optical quality and >500 nm thickness were produced in a single-spin coating step. The optimization of the procedure involves three crucial steps: the addition of an appropriate amount of PVP, O_2 plasma treatment to eliminate the formation of carbon deposits at the temperatures required to form the β-phase, and controlled temperature annealing. The resultant β-BBO films are highly orientated (006), and their thickness leads to an improved SHG efficiency compared to films produced without the addition of PVP.

The viscous gel precursor can be patterned by contact lithography. Both thick unpatterned and patterned β-BBO films arising from the results of this work are expected to find wide application in photonic devices and as nonlinear photonic crystals.

Acknowledgment. This work was supported by the Ontario Research and Development Fund through the Ontario Photonics Consortium, the Natural Science and Engineering Research Council of Canada (NSERC), and the University of Western Ontario. The authors thank Dr. Todd Simpson for his assistance in the UWO Nanofab and Professor Biswanath Mallik for his help in the measurements of the nonlinear coefficient of the BBO films.

CM071037M

(24) Prodan, L.; Euser, T. G.; van Wolferen, H. A. G. M.; Bostan, C.; de Ridder, R. M.; Beigang, R.; Boller, K. J.; Kuipers, L. *Nanotechnology* **2004**, *15*, 639.
(25) Chou, S. Y.; Keimel, C.; Gu, J. *Nature* **2002**, *417*, 835.